IEEE Access
Multidisciplinary | Rapid Review | Open Access Journal

Received 14 September 2022, accepted 25 September 2022, date of publication 27 September 2022,
date of current version 6 October 2022.

Digital Object Identifier 10.1109/ACCESS.2022.3210257

RESEARCH ARTICLE

Multi-Source DoA Estimation of EM Waves Impinging Spherical Antenna Array With Unknown Mutual Coupling Using Relative Signal Pressure Based Multiple Signal Classification Approach

OLUWOLE JOHN FAMORIJI, (Member, IEEE), AND THOKOZANI SHONGWE, (Senior Member, IEEE)
Department of Electrical and Electronic Engineering Technology, University of Johannesburg, Johannesburg 2006, South Africa
Corresponding author: Oluwole John Famoriji (famoriji@mail.ustc.edu.cn)

This work was supported in part by the University Research Committee (URC) of the University of Johannesburg, South Africa.

ABSTRACT Spherical antenna array (SAA) is a configuration that scans almost all the radiation sphere with constant directivity. It finds applications in spacecraft and satellite communication. Multiple signal classification (MUSIC) is a widely used multiple source direction-of-arrival (DoA) estimation method because of its low complexity implementation in practical applications. Conversely, it is susceptible to noise, which consequently affects its accuracy of localization. In this paper, MUSIC-based methods that operate at low signal-to-noise ratio (SNR) are developed via relative electromagnetic (EM) wave pressure measurements of a SAA. The proposed methods are the relative pressure MUSIC (RP-MUSIC), and in spherical domain (SH-RP-MUSIC). The developed SH-RP-MUSIC algorithm is in spherical domain thereby allows frequency-smoothing approach for the de-correlation of the coherent source signals towards an enhanced accuracy of localization. Both RP-MUSIC and SH-RP-MUSIC algorithms developed have the ability to estimate the number of active sources that is *a priori* knowledge of the conventional MUSIC algorithm. Numerical experiments were used to demonstrate the adequacy of the developed algorithms. In addition, measured data from experiment, which is the practically acceptable way to examine any procedure is employed to demonstrate the merits of the developed algorithms against the conventional MUSIC algorithm and other recent multiple source localization method in literature. Finally, in order to achieve DoA estimations with adequate localization accuracy at low SNR using SAA, SH-RP-MUSIC algorithm is a better choice.

INDEX TERMS DoA estimation, SAA, MUSIC, multiple source localization, relative signal pressure, estimation of number of source.

I. INTRODUCTION

Signal source localization is a crucial research subject matter in signal processing, due to its broad applications in signal enhancement and separation, signal detection, source tracking, camera steering, and signal recognition [1], [2], [3], [4], [5], [6]. Antenna arrays with distributed elements over a spherical surface satisfies the isotropic requirements. The spherical antenna array (SAA) as depicted in Figure 1 is an important array configuration, which has the ability to receive electromagnetic (EM) waves with the same strength independent of the polarization and direction-of-arrival (DoA) [3]. Exploring this merit of largest degree of freedom, SAA must be capable of determining the polarization and DoA of

The associate editor coordinating the review of this manuscript and approving it for publication was Gokhan Apaydin.

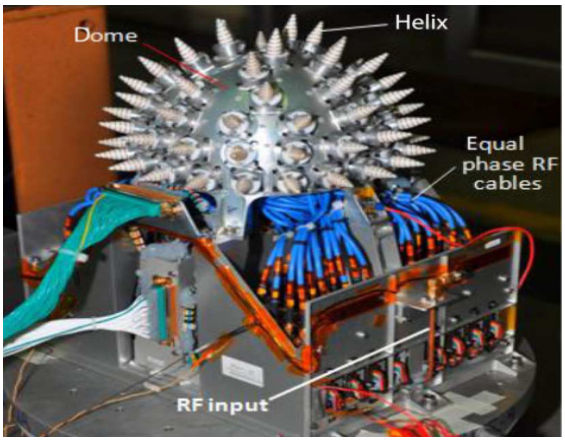

FIGURE 1. Picture of a mounted 64 elements spherical antenna array in an anechoic chamber [3].

incoming EM waves that impinge the unit sphere. Different theories have been presented to describe the SAA [5], [6], [7], [8], [9], [10], but accurate description and more insight of EM characteristics on SAA still require research attention.

Different DoA estimation methods that are useful in spherical harmonic (SH) domain have been reported in literature, such as, [7], [8], [9], and [10]. For example, SH decomposition has been used to represent coefficient-based reflected signals, mode strength matrix, and reflector locations [11]. Radial filters have been employed to separate sources that are located at different ranges from the system. Various methods have been proposed for radial filters [11], [12] using SH decomposition, but all the methods require priori knowledge of the DoA. Localization of sources of signals using SAA has hitherto not been investigated adequately at low signal-to-noise ratio (SNR). Multiple signal classification (MUSIC) has been widely used for DoA estimation, but it is susceptible to noise, which consequently affects its localization accuracy [2], [5], [10]. Hence, developing a DoA method for EM wave impinging SAA using relative signal pressure based multiple signal classification approach becomes important.

Furthermore, antenna arrays generally have different advantages, such as beamforming capacity, high gain, which are used for various mobile communications including controlled radiation pattern antenna for EM immunity to interference and military radar applications. However, the current trend in technology causes recent systems to be smaller, which lead to smaller space between elements in the array. This consequently lead to higher mutual coupling (MC) poor radiation features, and impedance mismatch. This challenge has severe effect on antenna array signal processing [8], [10]. Therefore, when estimating DoA of signals vis-à-vis antenna array, it is important to always consider the impact of MC on the system under consideration.

In the time past, DoA estimation has been conducted using estimation of subspace rotational in variance technology (ESPRIT) method, MUSIC, MUSIC group delay [11], [13], [14], steered response power with phase transform (SRP-PHAT) [15], [16], [17], [18], [19], [20], generalized cross-correlation (GCC) [21], adaptive eigenvalue decomposition [22], 1-D MUSIC [23], and order aware algorithm [24]. MUSIC has been considered in SH domain named as MUSIC-SH in [25], [26], and [27]. Due to the sensitivity of MUSIC-SH to distortion, Nakamura [28] proposed alternative method called direct-path dominance (DPD). In the near-field, strength of mode depends on the range of source, which is not known a priori. So, DPD is only demonstrated in time dimension, and as such, MUSIC-SH-DPD uses larger number of frames [28]. The minimum variance distortionless response is another DoA estimation algorithm in SH domain [29].

Lately, a 3-D source localization technique using cross array has been reported in [30]. This technique applies to various disallowed aperture loss and symmetric cross array. Shu *et al.* [31] used spatial spread vector element for three dimension (3-D) source localization. The technique can be applied to NLOS (non line of sight) propagations at an undefined exponent of path loss and provides improved estimation, as a result of the inherent expansion of spatial aperture in spread profile of the vector sensor. A low complex technique was achieved using orthogonal matching pursuit and discrete Fourier transform in [32]. This technique is robust at low SNR, and no matric decomposition is required. In addition, one snapshot localization method using discrete fractional Fourier transform has been proposed in [33] and [34]. This technique classifies and estimate mixed sources. An autocorrelation analysis and sources localization using cyclostationary features has been conducted in [35].

Another remedy to source solution at low SNR is to intuitively adopt source feature with lesser noise sensitivity. The relative transfer function (RTF), which is the ratio of signal transfer function (STF) of two radiating elements, is proven a potential source feature. RTF can be estimated via biased estimator that explore cross power spectral that exist between two elements [36], thereby makes it robust. Hence, recently developed source localization methods [36], [37], [38], [39], [40] and tracking methods [41], [42] have used it. RTF is source position dependent, due to its definition only at a signal source. Whereby, RTF is majorly employed to solve one-source localization problems [43], [44]. Lately, RTF dependent multiple source localization methods that perform pre-processing for the detection of the single source prior single source localization, have been proposed by Li *et al* [45], [46].

Contrary to past works in literature, the novelties of this paper are encapsulated as follows. Incited by RTF, this article describes the relative signal pressure as ratio of the signal pressure on the surface of SAA to the pressure at the origin. An approach with high level of robustness for the estimation of this quantity is presented. At far-field, the conventional MUSIC scheme is re-modeled employing relative pressure estimates as the input. The proposed technique (codenamed RP-MUSIC) is demonstrated to have the ability to estimate multi-source DoAs having appreciable level of robustness to noise. In addition, because of the relative signal pressure

with respect to origin is a normalized pressure, the presented scheme can be expressed in SH domain. Therefore, a relative signal pressure based SH MUSIC method (abbreviated as SH-RP-MUSIC) is proposed. This method has frequency-smoothing step for enhanced accuracy. SH-RP-MUSIC eases Bessel zero problem in open sphere because of its robustness to noise. Finally, both SH-RP-MUSIC and RP-MUSIC have another ability to estimate active signal sources when practical SNRs are present.

II. MATHEMATICAL FORMULATION OF SIGNAL MODEL

A. FORMULATION OF PROBLEM

Let us consider an SAA with M number of elements, having polar coordinates $\boldsymbol{x}_i = (r, \theta_i, \phi_i), i = 1, \ldots, M$, from the origin, as shown in Figure 2. Assuming there are V active sources situated at far field of SAA at angles $\varphi_i = (\theta_v, \phi_v), v = 1, \ldots, V$, with azimuth ϕ_v and inclination or elevation θ_v. Therefore, the pressure of signal at the *i-th* element in frequency domain is described as,

$$\begin{aligned}\bar{P}(\boldsymbol{x}_i, k) &= P(\boldsymbol{x}_i, k) + n(\boldsymbol{x}_i, k) \\ &= \sum_{v=1}^{V} s_v(k) e^{j\boldsymbol{k}_v^T \boldsymbol{x}_i} + n(\boldsymbol{x}_i, k) \end{aligned} \tag{1}$$

where k denotes the wave number ($k = 2\pi f / c$), c represents the speed of light, f is the frequency, $P(\boldsymbol{x}_i, k)$ and $\bar{P}(\boldsymbol{x}_i, k)$ are the noiseless and noisy pressure of signal, respectively. $s_v(k)$ is the *v-th* source signal detected from the origin, $n(\boldsymbol{x}_i, k)$ is additive noise present at *i-th* element, and the wavenumber is expressed as $\boldsymbol{k}_v = (kcos\phi_v sin\theta_v, ksin\phi_v sin\theta_v, kcos\theta_v)^T$. Note that Equation (1) assumes free field propagation, and expressed in form of vector as

$$\boldsymbol{P}(k) = \boldsymbol{G}(k)\boldsymbol{s}(k) + \boldsymbol{n}(k) \tag{2}$$

where $\boldsymbol{P}(k)$ represents a vector with size $M \times 1$ of signal pressure observed at the antennas, $\boldsymbol{n}(k)$ represents $M \times 1$ vector of noise, $\boldsymbol{s}(k)$ represents source signal vector $V \times 1$ of the signal source,

$$\boldsymbol{s}(k) = [s_1(k), s_2(k), \ldots, s_V(k)]^T. \tag{3}$$

The $\boldsymbol{G}(k)$ parameter in Equation (2) represents the $M \times V$ steering matrix,

$$\boldsymbol{G}(k) = \left[\boldsymbol{g}_1(k), \boldsymbol{g}_2(k), \ldots, \boldsymbol{g}_M(k)\right]^T \tag{4}$$

where $\boldsymbol{g}(k) = \left[e^{j\boldsymbol{k}_1^T \boldsymbol{x}_i}, e^{j\boldsymbol{k}_2^T \boldsymbol{x}_i}, \ldots, e^{j\boldsymbol{k}_V^T \boldsymbol{x}_i}\right]^T$ denotes the steering vector of antenna. Recall the additive noise in Eqn. (1) is considered as non-directional (with random white noise as an example), else, the directional noise is considered as added sources for localization. This article attempted the estimation of the unknown DoAs of entire signal sources, which are active i.e., $(\theta_v, \phi_v), v = 1, \ldots, V$, together with the estimation of number of signal source *V,* using noisy source data. Presently, the subspace MUSIC algorithm is a popular and often used method to resolve the problem. Conversely, the conventional MUSIC method suffers two main deficiencies.

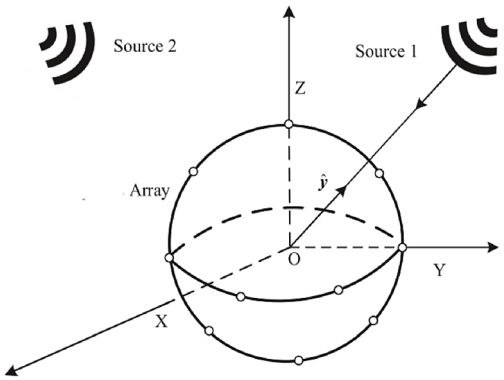

FIGURE 2. Estimation of multi-source DoA using SAA.

First is its sensitivity to noise, which severely impairs the accuracy of localization at low SNRs. The second drawback is the requirement of the number of source V to be known a priori, which is not available in practical scenario. Overcoming the aforementioned drawbacks, this article develops an enhanced MUSIC method that employs received signal termed relative signal pressure.

B. DESCRIPTION OF RELATIVE SIGNAL PRESSURE

The introduction of relative signal pressure (RSP) of SAA is given in this subsection. Considering the i-th antenna on SAA in Figure 2. The RSP associated with the signal pressure situated at the origin of the spherical array $\boldsymbol{x}_o = (0, 0, 0)$, can be expressed as

$$\boldsymbol{Q}(\boldsymbol{x}_i, k) = P(\mathbf{x}_i, k) / P(\mathbf{x}_o, k), \quad i = 1, \ldots, M \tag{5}$$

Equation (5) requires that the data is available at the origin. Conversely, some configured arrays, like rigid spherical arrays [47], have antennas on the surface of the array. In such case, the pressure is approximated at the origin of the array as a summation of all elements on the array surface as

$$P(\boldsymbol{x}_o, k) \approx \frac{1}{M} \sum_{i=1}^{M} P(\boldsymbol{x}_i, k). \tag{6}$$

Note, for single source, $V = 1$, the RSP of two elements equals its relative transfer function [43],

$$\boldsymbol{Q}(\boldsymbol{x}_i, k) = P(\mathbf{x}_i, k) / P(\mathbf{x}_o, k) = \frac{s(k) A(\boldsymbol{x}_i, k)}{s(k) A(\boldsymbol{x}_o, k)} = \frac{A(\boldsymbol{x}_i, k)}{A(\boldsymbol{x}_o, k)} \tag{7}$$

where $s(k)$ denotes the source signal, $A(\boldsymbol{x}_i, k)$ and $A(\boldsymbol{x}_o, k)$ denotes the transfer function of the EM wave emanated from the signal source to the elements, respectively, furthermore, $A(\boldsymbol{x}_i, k)$ and $A(\boldsymbol{x}_o, k)$ represents the relative transfer function between two elements. Conversely, the RSP is no longer associated with relative transfer function where $V > 1$ signal sources.

C. RSP ESTIMATION

To compute the RSP by the ratio of two antenna pressure containing significant errors at low SNRs, specifically when the denominator pressure of Eqn. (5) becomes low. In this subdivision, we overcome the problem by proposing another RSP estimate, where the two scenarios i.e. ideal (no noise scenario) and practical (with noise scenario) are considered The two scenarios are described as follows.

1) IDEAL SCENARIO (ENVIRONMENT WITHOUT NOISE)

The real description of Eqn. (5) is given as

$$Q\left(\boldsymbol{x}_i, k\right) = \frac{P\left(\boldsymbol{x}_i, k\right) P^*\left(\boldsymbol{x}_o, k\right)}{\left|P\left(\boldsymbol{x}_o, k\right)\right|^2}. \tag{8}$$

If the signal source is stationed or partially dynamic over a short period of time, then Eqn. (8) can be represented as

$$Q\left(\boldsymbol{x}_i, k\right) = \frac{S_{p_i p_o}(k)}{S_{p_o p_o}(k)} \tag{9}$$

where

$$S_{p_o p_o}(k) = \mathbb{E}\{P\left(\boldsymbol{x}_o, k\right) P^*\left(\boldsymbol{x}_o, k\right)\} \tag{10}$$

represents power spectral density of $P\left(\boldsymbol{x}_o, k\right)$, $\mathbb{E}\{\cdot\}$ is the operator of statistical expectation, and

$$S_{p_i p_o}(k) = \mathbb{E}\{P\left(\boldsymbol{x}_i, k\right) P^*\left(\boldsymbol{x}_o, k\right)\} \tag{11}$$

is the cross power spectral density between $P\left(\boldsymbol{x}_i, k\right)$ and $P\left(\boldsymbol{x}_o, k\right)$.

2) PRACTICAL SCENARIO (ENVIRONMENT WITH NOISE)

Substituting Eqn. (1) into Eqn. (9), the noisy RSP is

$$\bar{Q}\left(\boldsymbol{x}_i, k\right) = \frac{S_{\bar{p}_i \bar{p}_o}(k)}{S_{\bar{p}_o \bar{p}_o}(k)} \tag{12}$$

where $S_{\bar{p}_o \bar{p}_o}(k)$ and $S_{\bar{p}_i \bar{p}_o}(k)$ denotes noisy power spectral density and cross power spectral density, respectively. both $S_{\bar{p}_o \bar{p}_o}(k)$ and $S_{\bar{p}_i \bar{p}_o}(k)$ can further be expressed by adding components of noise and signal as

$$S_{\bar{p}_i \bar{p}_o}\left(k\right) - S_{p_i p_o}(k) S_{\bar{p}_o \bar{p}_o}\left(k\right) = S_{p_o p_o}\left(k\right) + S_{n_o n_o}(k) \tag{13}$$

where

$$S_{\bar{p}_i \bar{p}_o}\left(k\right) - S_{p_i p_o}(k) S_{n_o n_o}\left(k\right) = \mathbb{E}\{n\left(\boldsymbol{x}_o, k\right) n^*\left(\boldsymbol{x}_o, k\right)\} \tag{14}$$

represents the noise density of power spectrum at the pilot element. Eqn. (13) is with the assumption that the source signal and coherent noise signal are not correlated, in such a way that their cross power spectral density between the elements is zero. Putting Eqn. (13) into Eqn. (12), results to noisy RSP,

$$\bar{Q}\left(\boldsymbol{x}_i, k\right) = \frac{S_{p_i p_o}(k)}{S_{p_o p_o}\left(k\right) + S_{n_o n_o}\left(k\right)}. \tag{15}$$

If Eqn. (15) is divided by Eqn. (9), the following relationship between the noisy and noiseless RSP is derived as

$$\bar{Q}\left(\boldsymbol{x}_i, k\right) = Q(\boldsymbol{x}_i, k) \mathscr{P}(k) \tag{16}$$

where

$$\mathscr{P}(k) = \frac{T(\boldsymbol{x}_o, k)}{T\left(\boldsymbol{x}_o, k\right) + 1} \tag{17}$$

depends on SNR at the array origin, i.e. $T\left(\boldsymbol{x}_o, k\right) = S_{p_o p_o}\left(k\right) / S_{n_o n_o}\left(k\right)$, while the dependency of $\mathscr{P}(k)$ on $\boldsymbol{x}_o$ is neglected for easy computation. As we have in relative transfer function, the RSP expressed by the power spectral density between elements also show high level of robustness to noise.

III. RELATIVE SIGNAL PRESSURE BASED MUSIC

A method for the estimation of DoAs with RSP based on the conventional MUSIC approach scheme is outlined in this section.

A. RSP AT FAR FIELD

If we substitute the signal pressure by plane wave model into Eqn. (5), then the linear expression of RSP in an ideal environment is

$$\begin{aligned} Q\left(\boldsymbol{x}_i, k\right) &= \frac{\sum_{v=1}^{V} S_v(k) e^{-j\boldsymbol{k}_v^T \boldsymbol{x}_i}}{\sum_{v=1}^{V} S_v(k) e^{-j\boldsymbol{k}_v^T \boldsymbol{x}_o}} \\ &= \frac{\sum_{v=1}^{V} S_v(k) e^{-j\boldsymbol{k}_v^T \boldsymbol{x}_i}}{\sum_{v=1}^{V} S_v(k)} \\ &= \sum_{v=1}^{V} \bar{S}_v(k) e^{-j\boldsymbol{k}_v^T \boldsymbol{x}_i}, i = 1, \ldots, M \end{aligned} \tag{18}$$

where

$$\bar{S}_v(k) = \frac{S_v(k)}{\sum_{v=1}^{V} S_v(k)}, \tag{19}$$

Represents the component relative to the v-th source signal out of other sources. Eqn. (18) expressed as

$$Q\left(\boldsymbol{x}_i, k\right) = \boldsymbol{V}_i^T\left(k\right) \bar{s}(k) \tag{20}$$

where $\bar{s}(k)$ is a vector, $V \times 1$, expressed as

$$\bar{s}\left(k\right) = \left[\bar{s}_1\left(k\right), \bar{s}_2\left(k\right), \ldots, \bar{s}_V\left(k\right)\right]^T. \tag{21}$$

$\boldsymbol{V}_v(k)$ denotes steering vector. Putting Eqn. (20) into Eqn. (16), then the noisy RSP is expressed as

$$\bar{Q}\left(\boldsymbol{x}_i, k\right) = \boldsymbol{V}_i^T\left(k\right) \bar{s}\left(k\right) \mathscr{P}\left(k\right). \tag{22}$$

If we consider the entire M elements, Eqn. (22) is described in form of matrix,

$$\bar{Q}\left(k\right) = \boldsymbol{V}\left(k\right) \bar{s}\left(k\right) \mathscr{P}\left(k\right). \tag{23}$$

$\bar{\boldsymbol{Q}}\left(k\right)$ is the noisy RSP vector of all the channels of the antennas, $\boldsymbol{V}\left(k\right)$ is the steering matrix of Eqn. (4), and $\mathscr{P}(k)$ represents the scalar of Eqn. (17).

B. RP-MUSIC: MUSIC BASED ON RSP

The MUSIC method for the localization of multi-source is developed in this subsection using the RSP in Eqn. (23). Computing the noisy RSP $M \times M$ covariance matrix,

$$\boldsymbol{S}_{\bar{Q}}(k) = \mathbb{E}\{\bar{Q}(k)\,\bar{Q}^{H}(k) = \boldsymbol{V}(k)\boldsymbol{R}_{s}(k)\boldsymbol{V}^{H}(k)\} \quad (24)$$

where

$$\boldsymbol{R}_{\boldsymbol{S}}(k) = \mathbb{E}\{\bar{s}(k)\,\mathscr{P}(k)\bar{s}^{H}(k)\mathscr{P}^{*}(k)\} \quad (25)$$

is a matrix with full rank. In practical scenario, the eigenvectors that uses a SVD (singular value decomposition) of the covariance matrix can be obtained as

$$\boldsymbol{S}_{\bar{Q}}(k) = \begin{bmatrix}\bar{\boldsymbol{U}}_{s}\ \bar{\boldsymbol{U}}_{n}\end{bmatrix}\begin{bmatrix}\bar{\Sigma}_{s} & 0\\ 0 & 0\end{bmatrix}\begin{bmatrix}\bar{\boldsymbol{U}}_{s}^{H}\\ \bar{\boldsymbol{U}}_{n}^{H}\end{bmatrix} \quad (26)$$

for convenience sake, we omitted the frequency dependency. The covariance matrix of Eqn. (24) has no parameter that corresponds to noise, as compared with the conventional MUSIC algorithm. The analysis presented above demonstrated how the developed RP-MUSIC exhibits higher variation between the eigenvalue that corresponds to the subspaces of $\bar{U}_s$ and $\bar{U}_n$, respectively. Higher difference between the sorted eigenvalues makes the estimation of number of signal sources easier and does not require prior knowledge again. The step-by-step algorithm that considers wide band frequency is presented in Algorithm 1.

Algorithm 1 RP-Music

Input: Data or measurements in time domain.
Output: Estimation of DoA.

a) Transform the data to short-time Fourier transform domain.

b) Compute the RSP

c) Use eigenvalues for estimation of number of sources.

d) For $k = 1, 2, \ldots,$ do until:

1) Computation of covariance matrix $\boldsymbol{S_P}(\boldsymbol{k})$.

2) Subspace $\bar{U}_{\mathbf{n}}^{\mathbf{H}}$ computation using singular vector decomposition.

3) Over a particular space, calculate the pseudo spectrum,

$$\boldsymbol{M}\left(\boldsymbol{k},\boldsymbol{y_s}\right) = \frac{1}{\left\|\bar{U}_{\boldsymbol{n}}^{\boldsymbol{H}}(\boldsymbol{k})\boldsymbol{a}(\boldsymbol{k},\boldsymbol{y_s})\right\|^{2}}.$$

e) Spectrum averaging for a wide frequency band,

$$\tilde{M}\left(\boldsymbol{y_s}\right) = \frac{\mathbf{1}}{\boldsymbol{K}}\sum_{k\mathcal{D}\mathbf{1}}^{\mathbf{K}}\boldsymbol{M}\left(\mathbf{k},\mathbf{y_s}\right).$$

f) Searching of V peaks of the spectrum using $\tilde{M}$ to achieve the DoA.

IV. SH-RP-MUSIC: RSP BASED MUSIC IN SPHERICAL HARMONIC DOMAIN (SHD)

In this section, the developed RP-MUSIC method is transformed into SH-RP-MUSIC. This allows decorrelation of the coherent source signal using frequency smoothing towards enhanced accuracy of localization.

A. SHD

The RSP measurement over the antenna array, $\bar{Q}(\boldsymbol{x}_i, k)$, $i = 1, \ldots, M$, can be converted to SH domain by an orthogonal spatial functions [48],

$$\bar{Q}(\boldsymbol{x}_i, k) = \sum_{n=0}^{N}\sum_{m=-n}^{n}\bar{\beta}_{nm}(k)j_n(kr)Y_{nm}(\theta_i, \phi_i) \quad (27)$$

where m and $n(\geq 0)$ represent the integers, $\bar{\beta}_{nm}(k)$ denotes the SH coefficient, $j_n(\cdot)$ represents the spherical Bessel function, $N = \lceil kr \rceil$ denotes the truncated order [49],

$$Y_{nm}(\theta, \phi) = \sqrt{\frac{(2n+1)}{4\pi}\frac{(n-m)!}{(n+m)!}}P_{nm}(cos\theta)e^{jm\phi} \quad (28)$$

Eqn. (28) is the SH function, $P_{nm}(\cdot)$ represents the Legendre function. The coefficients of SH, $\bar{\beta}_{nm}(k)$, defining signal field in SH domain is measured by a SAA (M discrete antennas),

$$\bar{\beta}_{nm}(k) = \frac{1}{j_n(kr)}\sum_{i=1}^{M}a_i\bar{Q}(\boldsymbol{x}_i, k)\,Y_{nm}^{*}(\theta_i, \phi_i) \quad (29)$$

a_i is the weight of individual element ensuring orthogonality at the right side. The conventional SH decomposition of the noisy signal pressure, SH-MUSIC method [10], has Bessel zero problem because of the spherical Bessel function $j_n(kr)$ that is incorporated with little input for the output to tend towards zero crossings. As such, the component of noise in the SH coefficients measurement is highly amplified. In contrary, it results to lesser problem by the SH decomposition in Eqn. (29) because the sensitivity of the RSP to noise is lesser.

B. SH-RP-MUSIC IN CONJUNCTION WITH FREQUENCY SMOOTHING

The steering vector in Eqn. (22) associated with v-th signal source is transformable into SH domain [50], [51],

$$e^{-j\boldsymbol{k}_v^{T}x_i} = \sum_{n=0}^{N}\sum_{m=-n}^{n}4\pi i^{n}Y_{nm}^{*}(\varphi_v)j_n(kr)\,Y_{nm}(\theta_i, \phi_i). \quad (30)$$

If we substitute Eqns. (27) and (30) into Eqn. (22), the equation of the SH coefficients of the noisy RSP can be derived as

$$\bar{\beta}_{nm}(k) = \boldsymbol{y}_{nm}(k)\bar{\boldsymbol{s}}(k)\,\mathscr{P}(k) \quad (31)$$

$\bar{\boldsymbol{s}}(k)$ represents the vector of Eqn. (21), $\boldsymbol{y}_{nm}(k)$ denotes the steering vector at degree m and order n associated with each source,

$$\boldsymbol{y}_{nm}(k) = 4\pi\left[i^{n}Y_{nm}^{*}(\varphi_1), i^{n}Y_{nm}^{*}(\varphi_2), \ldots, i^{n}Y_{nm}^{*}(\varphi_V)\right]. \quad (32)$$

It can be noted that Eqn. (31) has only one SH mode. If all cases associated to the N-th order are combined, then Eqn. (32) can be written in form of matrix

$$\bar{\mathfrak{B}}(k) = \boldsymbol{Y}(k)\bar{\boldsymbol{s}}(k)\,\mathscr{P}(k) \quad (33)$$

where $\boldsymbol{Y}(k)$ represents the $(N+1)^2 \times V$ steering matrix in SH domain,

$$\boldsymbol{Y}(k) = \left[\mathbf{y}_{00}(k), \mathbf{y}_{1,-1}(k), \ldots, \mathbf{y}_{NN}(k)\right]^T. \quad (34)$$

The matrix of correlation of noisy SH coefficients over a source time-dependent source signal is described as

$$\boldsymbol{S}_{\bar{\mathfrak{B}}} = \mathbb{E}\{\bar{\mathfrak{B}}(k)\,\bar{\mathfrak{B}}^H(k)\} = \boldsymbol{Y}(k)\boldsymbol{R}_{\boldsymbol{S}}(k)\boldsymbol{Y}^H(k) \quad (35)$$

where $\boldsymbol{R}_{\boldsymbol{S}}(k)$ and $\boldsymbol{Y}(k)$ denote covariance matrix and steering matrix that have frequency and angular parts, correspondingly. The MUSIC method assumed $\boldsymbol{R}_{\boldsymbol{S}}(k)$ matrix in full rank. Conversely, such supposition may not align with practical because multi-source data may be coherent as

$$rank\ \boldsymbol{R}_{\boldsymbol{S}}(k) < V. \quad (36)$$

It is a general merit that both angular varying and frequency varying components are uncoupled in SH domain. Therefore, the source signal (coherent) is decorrelated via the implementation of the frequency smoothing, which calculate the covariance matrix (smoothed) to be medial of the covariance matrices at various bands of frequency [50],

$$\tilde{\boldsymbol{S}}_{\boldsymbol{P}} = \frac{1}{K}\sum_{k=1}^{K}\boldsymbol{S}_{\bar{\mathfrak{B}}}(k) = \boldsymbol{Y}(k)\tilde{R}_{\boldsymbol{S}}(k)\,\boldsymbol{Y}^H(k) \quad (37)$$

where

$$\tilde{R}_{\boldsymbol{S}}(k) = \frac{1}{K}\sum_{k=1}^{K}\boldsymbol{R}_{\boldsymbol{S}}(k) \quad (38)$$

where frequency bins K were explored. In addition, we decomposed the smoothed covariance matrix by the use of SVD, and pseudo-spectrum is computed in order to end the estimation of DoA from multiple sources. The systematic step-by-step of SH-RP-MUSIC approach is presented in Algorithm 2.

Algorithm 2 SH-RP-Music

Input: Data or measurements in time domain.
Output: Estimation of DoA.

a) Transform the data to STFT domain.
b) Compute the RSP
c) Compute the coefficients of SH.
d) For $k = 1, 2, \ldots,$ do up to:
e) Computation of covariance matrix $\mathbf{S}_{\bar{\mathfrak{B}}}(\mathbf{k})$.
f) Compute the smoothed covariance matrix,

$$\tilde{\boldsymbol{S}}_{\boldsymbol{P}} = \frac{\mathbf{1}}{\boldsymbol{K}}\sum_{\boldsymbol{k}=1}^{\boldsymbol{K}}\boldsymbol{S}_{\bar{\mathfrak{B}}}(\boldsymbol{k}).$$

g) Use eigenvalue to compute the number of sources.
h) Compute the subspace $\mathbf{U_n}$.
i) Compute pseudo-spectrum $\tilde{M}(\mathbf{y_s})$.
j) Searching of V peaks of the spectrum using $\tilde{M}$ to achieve the DoA.

V. NUMERICAL EXPERIMENT, RESULTS, AND DISCUSSION

In this section, the evaluation and analysis of the developed RP-MUSIC and SH-RP-MUSIC algorithms are presented. Different numerical simulation scenarios were conducted to test the effectiveness of the developed methods as presented in Algorithms 1 and 2 accordingly. In addition, measured data from experiment, which in the end, is the ground truth to test any procedure are also used to demonstrate the effectiveness of RP-MUSIC and SH-RP-MUSIC.

A. SIMULATION DATA

A 32-element SAA of radius 4.2 cm and operating at 8 GHz, is simulated using CST as contained in [2]. Some active sources are simultaneously active. The incoming signals are measured by the SAA. An open spherical array was used for convenience, but the proposed method can be extended to rigid arrays directly whenever the scattering factor is added to the method. Data were generated from the CST [2] while RP-MUSIC and SH-RP-MUSIC were implemented in Matlab 2021b. The time domain data generated are observed using the SAA, and are impaired by noise that is randomly generated at all the elements on the array. STFT was employed to transform the data to frequency domain. Sixteen SH modes corresponding to third order $N = \lceil kr \rceil$ are used by the RP-MUSIC and SH-RP-MUSIC algorithms. While computing the RSP, it is assumed that the EM wave is not moving for around 0.1 s. Welch algorithm [52] is utilized for the calculation of the power spectral density and cross power spectral density using 0.017 s windows with 50% overlap.

B. PERFORMANCE METRICS AND BASELINE APPROACHES

RP-MUSIC and SH-RP-MUSIC methods are evaluated and compared with three multiple source localization methods using source feature of the relative harmonic coefficients. The three methods are (a) conventional SHD-MUSIC [53], (b) signal pressure based MUSIC in [54], and (c) the method developed in [52]. For convenience sake, the MUSIC based methods are abbreviated to RP-MUSIC, SH-RP-MUSIC, SH-MUSIC, and MUSIC. The other method in [52] is appreciably non-identical with the MUSIC dependent approaches because it uses a pre-processing method for components detection where a source is active. Principally, all the methods of localization in this paper samples 2-D space. The azimuth and elevation grids are divided (ensuring uniformity) into 90 samples to achieve total sum of 8100 samples.

The experiments that follow implement the methods until $\mathcal{N}_{tot} > 1$ times for consistency in the results. Each test employs the signal sources situated at randomly observed DoAs. Two qualitative metrics were used to evaluate the performance of the methods. First is the success ratio (SR), defined as

$$SR = \frac{\mathcal{N}_{sus}}{\mathcal{N}_{tot}} \times 100\% \quad (39)$$

TABLE 1. Distortion of signal pressure and RSP at different SNRs using Eqns. (41) and (42).

Error	SNRs (dB)				
	5	10	15	20	25
$Error_{\Lambda_Q}$	-0.50	-1.48	-3.12	-5.23	-7.74
$Error_{\Lambda_P}$	11.16	8.69	6.17	3.68	1.22

where $\mathcal{N}_{sus}$ represents the number of event that were detected successfully for the entire V sources. Bigger SR implies that the method has bigger capability for sources localization in the condition. The second metric is MAEE (mean absolute estimated error) between the estimate and actual DoAs. It can be expressed as

$$MAEE = \frac{1}{2V\mathcal{N}_{sus}} \left(\sum_{m=1}^{\mathcal{N}_{sus}} \sum_{v=1}^{V} \left| \theta_{act}^{m}(v) - \theta_{esti}^{m}(v) \right| + \left| \theta_{act}^{m}(v) - \theta_{esti}^{m}(v) \right| \right). \quad (40)$$

It is the measurement of the average numerical accuracy over the $\mathcal{N}_{sus}$.

C. VERIFICATION

Using the data obtained from simulations, we can compute the distortion over STFT as

$$Error_{\Lambda_P} = 10\log_{10}\left(\frac{1}{MTF}\sum_{t=1}^{T}\sum_{k=1}^{F}\sum_{i=1}^{M}\Lambda_{P_t(\boldsymbol{x}_i,k)}\right) \quad (41)$$

$$Error_{\Lambda_Q} = 10\log_{10}\left(\frac{1}{MTF}\sum_{t=1}^{T}\sum_{k=1}^{F}\sum_{i=1}^{M}\Lambda_{Q_t(\boldsymbol{x}_i,k)}\right) \quad (42)$$

where M, F, and T represent total elements of the array, frequency bins, and time, respectively, while i, k, and t are the respective index number. The errors associated with RSP and direct signal pressure (DSP), at different SNRs are presented in Table 1. Each figure in the Table is an average of five tests conducted. It can be seen that the measurement of RSP and pressure exhibit higher distortions as the SNR reduces. Conversely, it can be observed that the distortion of RSP is around 9 dB lesser than the signal pressure, which is an indication of an enhanced robustness to noise.

D. ACTIVE SOURCES ESTIMATION

Based on Eqn. (26), the higher the variation between the computed eigenvalues enhances the number of signal sources estimation. Before analyzing the accuracy of localization, at first, we can estimate the number of unknown source from the available multiple source data. Considering the four MUSIC based algorithms, the normalized eigenvalues are as depicted in Figure 3. The original condition is one with 3 signal sources having the elevation and azimuth $(150^0, 260^0)$, $(31^0, 69^0)$, $(96^0, 102^0)$, respectively. The eigenvalues for RP-MUSIC and MUSIC are set at 32, implying the total number of antennas. In contrary, the dimensions of SH-RP-MUSIC and SH-MUSIC are the total SH modes, which is 16. It can be observed that the eigenvalues associated with RP-MUSIC exhibits relatively wide gap between the third and fourth ones, implying three sources. Conversely, the difference that exist between the third and fourth eigenvalues of the signal pressure is obviously lesser. The issue is higher in the SH domain, where the developed SH-RP-MUSIC exhibit higher differences between the third and fourth eigenvalues. It can be pointed out that the developed algorithms enhance the number of source estimation under a condition. However, it cannot be ensured that a correct estimate can be achieved at lower SNRs (for instance, 5 dB), hence, source number prior knowledge at very low SNRs remains a requirements.

E. DoA ESTIMATION UNDER DIFFERENT SCENARIOS

The developed algorithms assume far-field scenario. Therefore, it becomes important to examine the effect of multi-source to element distance on the developed algorithms. When the distances are increased, other dimension (i.e. length, width, and height) are increased. Three signal sources having $(42^0, 26^0)$, $(18^0, 252^0)$, $(147^0, 220^0)$, elevation and azimuth, respectively, were simulated. The SAA remains in the same positions, having distances from 3 m to 5 m between the antenna array. The analysis was implemented at 30 dB SNR. When the distance was varied, the MAEE is at 1^0, which is a testimony and confirmation of far-field assumption is holding generally.

Furthermore, to evaluate the impact of different SNRs on the proposed methods, three signal sources with elevation and azimuth angles $(109^0, 305^0)$, $(62^0, 95^0)$, $(125^0, 175^0)$, respectively, were simulated. The multiple source data is measured at 10 dB and 30 dB SNR levels and the pseudo-spectrum is plotted directly. Under all the cases, the RP-MUSIC algorithm exhibits better performance with 3 evident peaks (i.e. the source DoAs detected). Contrary to the RP-MUSIC, the SH-RP-MUSIC shows sharper peaks. Conversely, at 10 dB, SH-RP-MUSIC did not localize the three sources as shown in Figure 4, this is due to higher sensitivity of SH-RP-MUSIC to noise as a result of Bessel zero problem.

F. PROPOSED METHODS VERSUS THE CONVENTIONAL MUSIC APPROACHES

In this subsection, the developed MUSIC based methods are compared with the conventional MUSIC methods. The conventional SH-MUSIC in [53] equally employs frequency smoothing. Therefore, the 4 MUSIC methods are implemented using 50 measured data in which multiple sources randomly propagate from chosen set of DoA.

All the approaches are evaluated at different SNRs. Table 2 and Table 3 show the performance at the 10 dB to 30 dB SNRs. It is noticed how localization accuracy degrades as SNR decreases. The developed RP-MUSIC algorithm

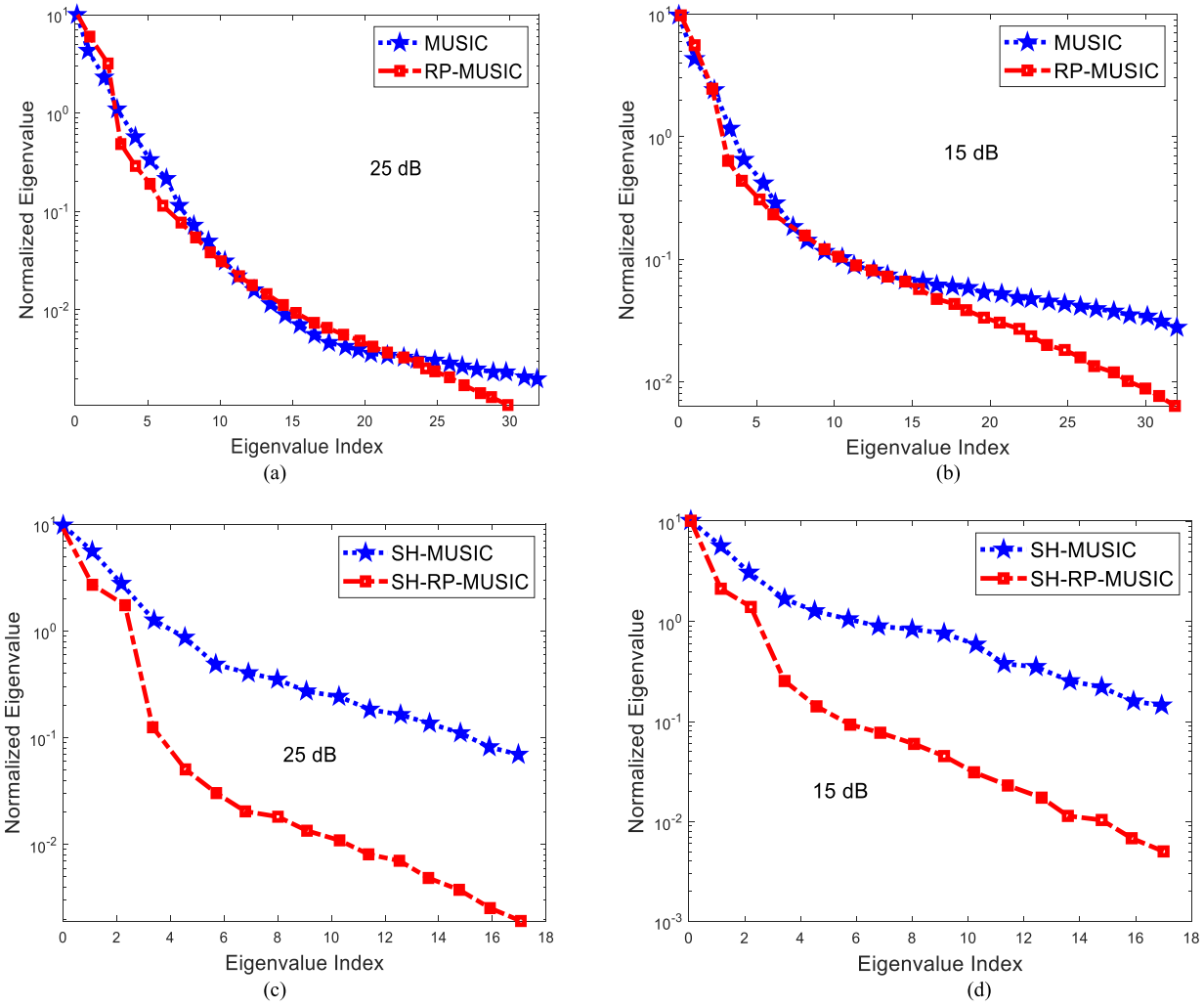

FIGURE 3. Eigenvalues (normalized) computed using SVD of covariance matrix of the source signal. (a) MUSIC and RP-MUSIC at 25 dB SNR, (b) MUSIC and RP-MUSIC at 15 dB SNR, (c) SH-MUSIC and SH-RP-MUSIC at 25 dB SNR, (d) SH-MUSIC and SH-RP-MUSIC at 15 dB SNR.

exhibits close performance with or more worse than the MUSIC algorithm at 10 dB SNR. The reason could be attributed to the associated assumption of the developed RP-MUSIC algorithm may not be valid at lower SNRs. Conversely, in most scenarios, an enhanced level of robustness of RP-MUSIC and SH-RP-MUSIC is observed, as against MUSIC and the SH-MUSIC. In conclusion, the results here demonstrate how the developed methods perform better than the conventional methods. Specifically, the SH-RP-MUSIC perform better than other methods under almost all cases, with a success ratio of about 93% and a MAEE less than 4^0.

The developed algorithms exhibit enhanced accuracy of localization at the expense of higher computational cost or complexity in computation. This is due to RSP computation. For verification, the complexity is measured via direct estimate of time cost over 10 concurrent scenarios, employing Matlab installed on a personal computer (PC); Intel CPU, Core i7-8565U, 8^{th} Gen., RAM 16 GB, 1 Terabyte. For a 4 sec. long measurement, the time taken (in term of run time) by both MUSIC and SH-MUSIC methods are 3.2 s and 5.9 s, respectively. In contrary, the time taken by RP-MUSIC and SH-RP-MUSIC methods are 4.8 s and 7.8 s, respectively. SH-MUSIC and SH-RP-MUSIC methods take longer time than MUSIC and RP-MUSIC algorithms, due to expensive transformation of the array signals into SH domain.

G. MULTIPLE SOURCE LOCALIZATION METHOD DEVELOPED IN [52] VERSUS THE PROPOSED METHODS

The developed MUSIC based methods concurrent multiple source data. In this subsection, the developed methods are compared with another kind of technique in [52]. The reference [52] is used as baseline. This method is made up of two steps. The first step implements the pre-processing stage for the detection of single source STFT bins. Furthermore, a single source localization is implemented for a specific single source STFT bins detected. The above investigations

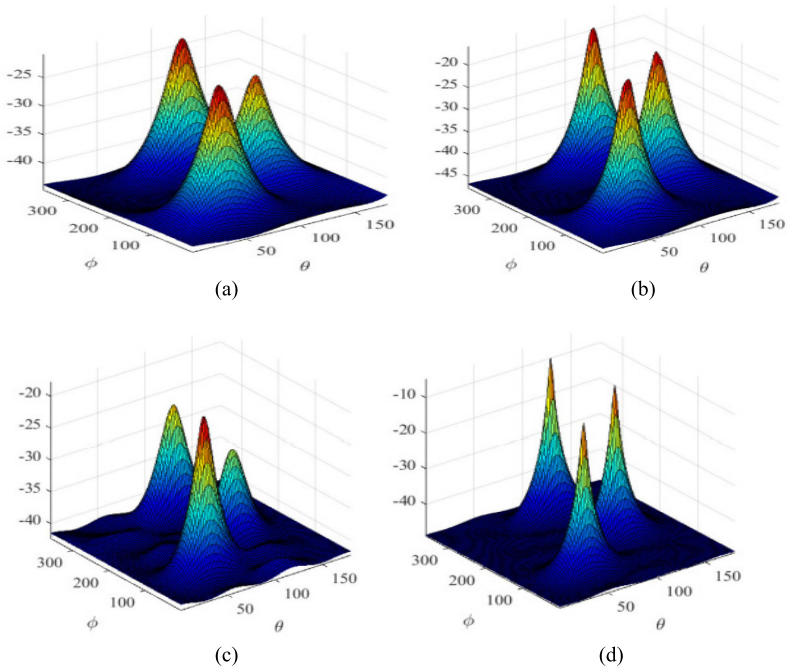

FIGURE 4. Three signal sources pseudo-spectrum plots using the developed algorithms. (a) RP-MUSIC at 10 dB, (b) RP-MUSIC at 30 dB, (c) SH-RP-MUSIC at 10 dB, and (d) SH-RP-MUSIC at 30 dB.

TABLE 2. Multiple source localization error at different SNRs using MAEE metric in Eqn. (40).

MAEE of Techniques	SNR (dB)		
	10	20	30
MUSIC	1.80	1.69	1.68
RP-MUSIC	1.92	1.66	1.61
SH-MUSIC	3.60	1.76	1.70
SH-RP-MUSIC	3.85	1.83	1.56

TABLE 3. Multiple source localization error at different SNRs using SR in Eqn. (39) metric.

SR of Techniques	SNR (dB)		
	10	20	30
MUSIC	0.95	0.95	0.95
RP-MUSIC	0.95	0.99	0.99
SH-MUSIC	0.89	1.05	1.05
SH-RP-MUSIC	1.01	1.09	1.09

employs source data obtained from 3 sources only. In this article, various source numbers are taken into account. Table 4 and 5 show the MAEEs of each method at 20 dB. The results in the Table are calculated with 50 measurements. Evidently, the success ratio reduces as the source's number increases. Specifically, at 4 source's number, there is degradation in the developed RP-MUSIC. This is due to difficulty in differentiating the adjacent sources for a bigger number of sources within the neighborhood. There is degradation in the baseline method for larger number of sources due to the remaining less single source bins or frames accessible for the localization of single source. Tables 4 and 5 show that the developed methods, particularly the SH-RP-MUSIC performs better than the baseline method under most cases.

H. VERIFICATION WITH MEASURED DATA FROM EXPERIMENT

Here, the measured data obtained from experiment is used for the validation and efficiency of the developed methods in practice. The experiment was conducted according to [10] to incorporate mutual coupling effect [9], [55]. The fabricated SAA is adopted [3] built to generate multiple source data. The SAA is an antenna array with reflection generated on its surface, and are not negligible. Hence, the measurement of SH coefficient in Eqn. (29) has to be modified [56] as

$$\bar{\beta}_{nm}(k) = \frac{1}{b_n(kr)} \sum_{i=1}^{M} a_i \bar{Q}(\boldsymbol{x}_i, k)\, Y_{nm}^{*}(\theta_i, \phi_i) \tag{43}$$

TABLE 4. Multiple source localization error with different number of sources using MAEE metric.

MAEE of Techniques	Sources		
	2	3	4
Baseline [52]	4.33	3.44	2.91
RP-MUSIC	1.67	1.61	1.80
SH-RP-MUSIC	1.36	1.47	2.28

TABLE 5. Multiple source localization error with different number of sources using SR metric.

MAEE of Techniques	Sources		
	2	3	4
Baseline [52]	1.01	0.99	0.93
RP-MUSIC	1.07	0.99	0.75
SH-RP-MUSIC	1.11	1.07	0.99

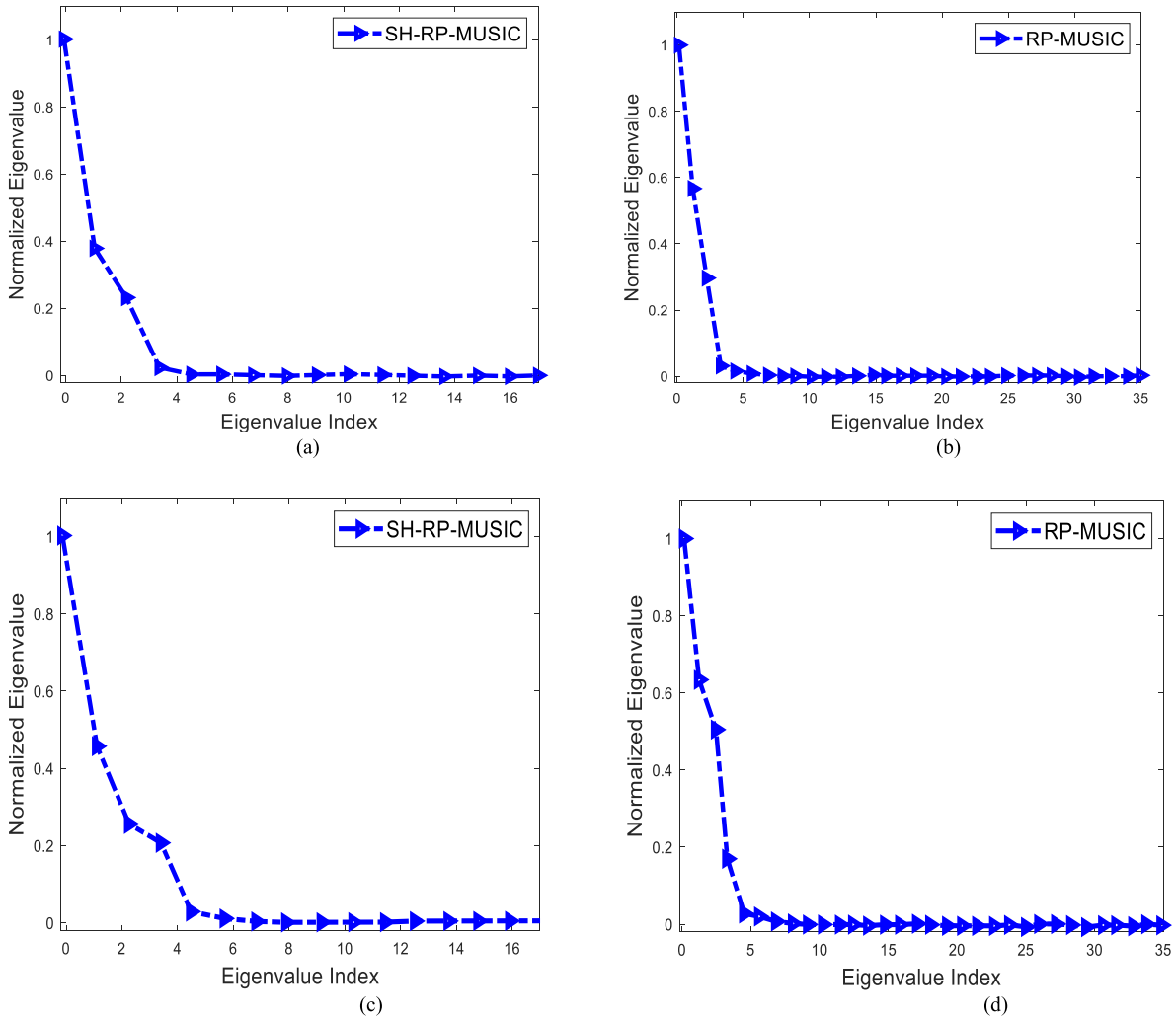

FIGURE 5. Normalized eigenvalues computed using measurements. (a) SH-RP-MUSIC with 3 sources, (b) RP-MUSIC with 3 sources, (c) SH-RP-MUSIC with 4 sources, and (d) RP-MUSIC with 4 sources.

where

$$b_n(kr) = j_n(kr) - \frac{j_n'(kR)}{h_n'(kR)} h_n(kr) \tag{44}$$

R denotes the antenna array radius, $j_n'(\cdot)$ and $h_n'(\cdot)$ are the partial derivative of spherical Bessel and Hankel function, correspondingly.

The proposed methods employ similar parameter setting as indicated in the simulation scenarios for the processing of measured data. At first, we computed the number of source via eigenvalues calculation via the developed algorithms. The number of sources under consideration are 3, and 4. The instances of the sorted eigenvalues for 3 and 4 sources are presented in Figure 5. The actual number of source is easily

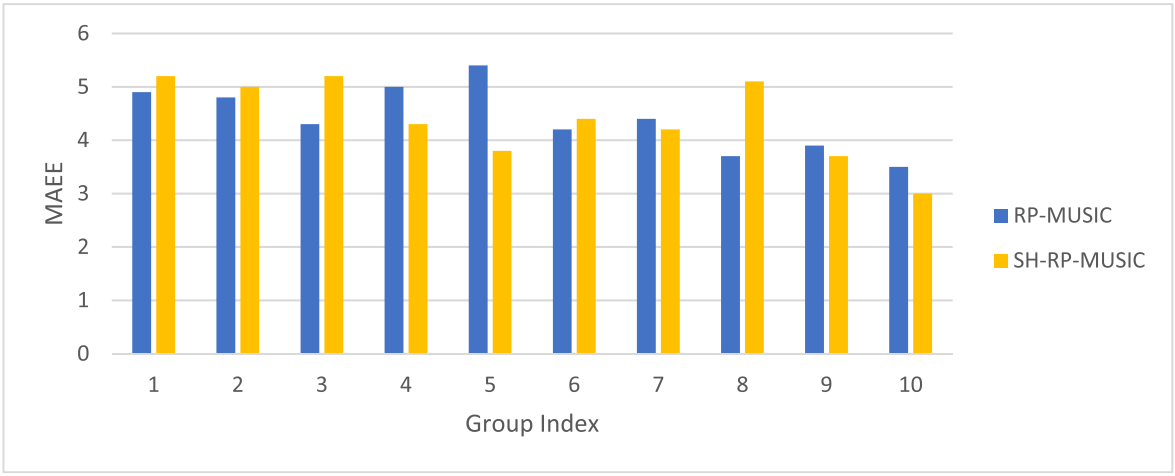

(a)

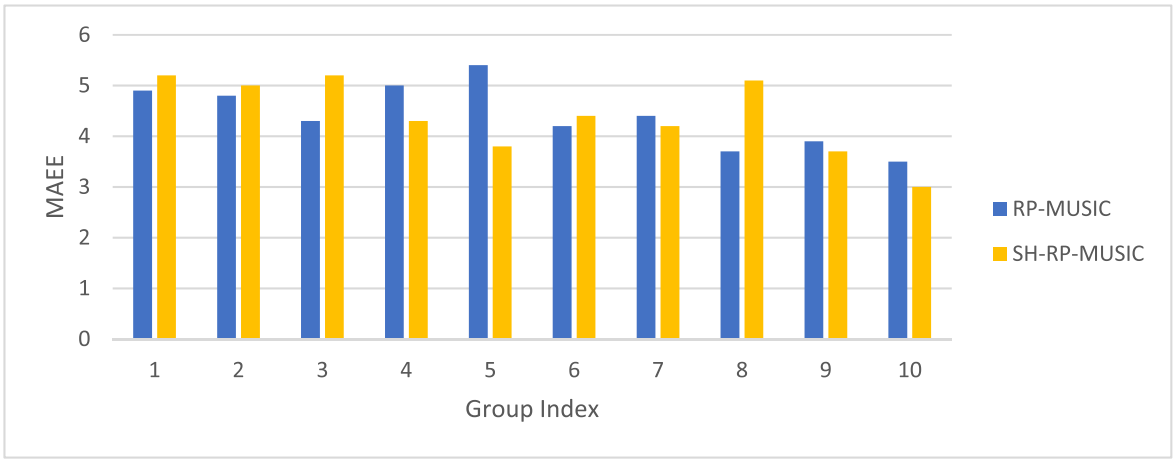

(b)

FIGURE 6. MAEE Performance of the developed technique using measurements. (a) 3 EM wave sources, (b) 4 EM wave sources.

estimated via the sorted eigenvalues. Secondly, the accuracy of localization is evaluated. For each scenarios, 10 instances of randomly chosen units from the SAA in Figure 3 are employed for measurements. The MAEE computed for each scenario is presented in Figure 6. The average MAEE for 10 scenarios is around 6^0, which shows that the developed algorithms successfully estimate the DoAs of the source. The accuracy level of measurement based estimation exhibits bigger errors than that of the simulation data. This is because the measurement is practical having non-negligible errors, such as measurement and position errors.

VI. CONCLUSION AND FUTURE WORK

In this paper, multi-source DoA estimation of EM wave impinging SAA under noisy scenario using RSP based MUSIC method in SH domain has been proposed. During the decomposition of the developed method, a frequency smoothing method is made for coherent source signals decorrelation towards enhanced accuracy. Performance evaluation under different conditions using numerical simulations demonstrates the accuracy enhancement and effectiveness when compared with the conventional methods at the expense of small computational cost. Moreover, measured data from experiment, which is the practical truth to examine any procedure shows that the proposed RP-MUSIC and SH-RP-MUSIC methods are motivating enough for practical applications.

In spite of the results emanated from this work, there are still issues begging for research attentions. For instance, at lower level (at about $\leq$5 dB) of SNR, both RP-MUSIC and SH-RP-MUSIC methods are unable to perform efficiently. One of the possible solutions to be considered in the future is to come up with EM signal feature using RSP and use it as input to a learning scheme (convolutional neural network), so as to attain enough accuracy of localization under the severely low SNRs.

REFERENCES

[1] M. Carlin, P. Rocca, G. Oliveri, F. Viani, and A. Massa, "Directions-of-arrival estimation through Bayesian compressive sensing strategies," *IEEE Trans. Antennas Propag.*, vol. 61, no. 7, pp. 3828–3838, Jul. 2013.

[2] M. G. Pralon, G. Del Galdo, M. Landmann, M. A. Hein, and R. S. Thoma, "Suitability of compact antenna arrays for direction-of-arrival estimation," *IEEE Trans. Antennas Propag.*, vol. 65, no. 12, pp. 7244–7256, Dec. 2017.
[3] B. P. Kumar, C. Kumar, V. S. Kumar, and V. V. Srinivasan, "Active spherical phased array design for satellite payload data transmission," *IEEE Trans. Antennas Propag.*, vol. 63, no. 11, pp. 4783–4791, Nov. 2015.
[4] P. Knott, "Design and experimental results of a spherical antenna array for a conformal array demonstrator," in *Proc. 2nd Int. ITG Conf. Antennas*, Mar. 2007, pp. 1–4.
[5] S. Tervo and A. Politis, "Direction of arrival estimation of reflections from room impulse responses using a spherical microphone array," *IEEE/ACM Trans. Audio, Speech, Language Process.*, vol. 23, no. 10, pp. 1539–1551, Oct. 2015.
[6] Y. Hu, T. D. Abhayapala, and P. N. Samarasinghe, "Multiple source direction of arrival estimations using relative sound pressure based MUSIC," *IEEE/ACM Trans. Audio, Speech, Language Process.*, vol. 29, pp. 253–264, Nov. 2021.
[7] O. J. Famoriji and T. Shongwe, "Direction-of-arrival estimation of electromagnetic wave impinging on spherical antenna array in the presence of mutual coupling using a multiple signal classification method," *Electronics*, vol. 10, no. 2651, pp. 1–15, 2021.
[8] O. J. Famoriji and T. Shongwe, "Source localization of EM waves in the near-field of spherical antenna array in the presence of unknown mutual coupling," *Wireless Commun. Mobile Comput.*, vol. 2021, pp. 1–14, Dec. 2021.
[9] O. J. Famoriji and T. Shongwe, "Critical review of basic methods on DoA estimation of EM waves impinging a spherical antenna array," *Electronics*, vol. 11, pp. 1–25, Jan. 2022.
[10] O. J. Famoriji, O. Y. Ogundepo, and X. Qi, "An intelligent deep learning-based direction-of-arrival estimation scheme using spherical antenna array with unknown mutual coupling," *IEEE Access*, vol. 8, pp. 179259–179271, 2020.
[11] I. Agrawal and R. M. Hegde, "Radial filters for near field source separation in spherical harmonic domain," in *Proc. IEEE Int. Conf. Acoust., Speech Signal Process. (ICASSP)*, Mar. 2016, pp. 116–120.
[12] E. Fisher and B. Rafaely, "Near-field spherical microphone array processing with radial filtering," *IEEE Trans. Audio, Speech, Language Process.*, vol. 19, no. 2, pp. 256–265, Feb. 2011.
[13] Z. Huang, W. Wang, F. Dong, and D. Wang, "A one-snapshot localization algorithm for mixed far-field and near-field sources," *IEEE Commun. Lett.*, vol. 24, no. 5, pp. 1010–1014, May 2020.
[14] Y. Kuznetsov, A. Baev, M. Konovalyuk, A. Gorbunova, and J. A. Russer, "Autocorrelation analysis and near-field localization of the radiating sources with cyclostationary properties," *IEEE Trans. Electromagn. Compat.*, vol. 62, no. 5, pp. 2186–2195, Oct. 2020.
[15] C. Knapp and G. Carter, "The generalized correlation method for estimation of time delay," *IEEE Trans. Acoust., Speech, Signal Process.*, vol. ASSP-24, no. 4, pp. 320–327, Aug. 1976.
[16] M. S. Brandstein and H. F. Silverman, "A robust method for speech signal time-delay estimation in reverberant rooms," in *Proc. IEEE Int. Conf. Acoust., Speech, Signal Process.*, Apr. 1997, pp. 375–378.
[17] A. Johansson, G. Cook, and S. Nordholm, "Acoustic direction of arrival estimation, a comparison between root-music and SRP-PHAT," in *Proc. IEEE TENCON*. Chiang Mai, Thailand, Nov. 2004, pp. 629–632.
[18] L. Kumar, A. Tripathy, and R. M. Hegde, "Robust multi-source localization over planar arrays using MUSIC-group delay spectrum," *IEEE Trans. Signal Process.*, vol. 62, no. 17, pp. 4627–4636, Sep. 2014.
[19] V. Varanasi and R. Hegde, "Robust online direction of arrival estimation using low dimensional spherical harmonic features," in *Proc. IEEE Int. Conf. Acoust., Speech Signal Process. (ICASSP)*, Mar. 2017, pp. 511–515.
[20] Y. Huang, J. Benesty, and G. W. Elko, "Adaptive eigenvalue decomposition algorithm for real time acoustic source localization system," in *Proc. IEEE Int. Conf. Acoust., Speech, Signal Processing. (ICASSP)*, Mar. 1999, pp. 937–940.
[21] C. Zhang, D. Florencio, and Z. Zhang, "Why does PHAT work well in lownoise, reverberative environments?" in *Proc. IEEE Int. Conf. Acoust., Speech Signal Process.*, Mar. 2008, pp. 2565–2568.
[22] E. Fisher and B. Rafaely, "The nearfield spherical microphone array," in *Proc. IEEE Int. Conf. Acoust., Speech Signal Process.*, Mar. 2008, pp. 5272–5275.
[23] Q. Huang and T. Chen, "One-dimensional MUSIC-type algorithm for spherical microphone arrays," *IEEE Access*, vol. 8, pp. 28178–28187, 2020.
[24] W. Gao and H. Chen, "An order-aware scheme for robust direction of arrival estimation in the spherical harmonic domain," *J. Acoust. Soc. Amer.*, vol. 146, no. 6, p. 4883, 2019.
[25] Y. R. Zheng, R. A. Goubran, and M. El-Tanany, "Robust near-field adaptive beamforming with distance discrimination," *IEEE Trans. Speech Audio Process.*, vol. 12, no. 5, pp. 478–488, Sep. 2004.
[26] F. Jacobsen, G. Moreno-Pescador, E. Fernandez-Grande, and J. Hald, "Near field acoustic holography with microphones on a rigid sphere (L)," *J. Acoust. Soc. Amer.*, vol. 129, no. 6, pp. 3461–3464, Jun. 2011.
[27] B. Rafaely, "Spatial sampling and beamforming for spherical microphone arrays," in *Proc. Hands-Free Speech Commun. Microphone Arrays*, May 2008, pp. 5–8.
[28] S. Nakamura, "Acoustic sound database collected for hands-free speech recognition and sound scene understanding," in *Proc. Int. Workshop Hands-Free Speech Commun.* Baixas, France, 2001, pp. 43–46.
[29] R. Takeda and K. Komatani, "Sound source localization based on deep neural networks with directional activate function exploiting phase information," in *Proc. IEEE Int. Conf. Acoust., Speech Signal Process. (ICASSP)*, Mar. 2016, pp. 405–409.
[30] X. Wu and J. Yan, "3-D mixed far-field and near-field source localization," *IEEE Trans. Veh. Technol.*, vol. 69, no. 6, pp. 6833–6837, Apr. 2020.
[31] T. Shu, J. He, and V. Dakulagi, "3-D near-field source localization using a spatially spread acoustic vector sensor," *IEEE Trans. Aerosp. Electron. Syst.*, vol. 58, no. 1, pp. 180–188, Feb. 2022.
[32] G. Liu and X. Sun, "Efficient method of passive localization for mixed far-field and near-field sources," *IEEE Antennas Wireless Propag. Lett.*, vol. 12, pp. 902–905, 2013.
[33] Z. Huang, B. Xue, W. Wang, F. Dong, and D. Wang, "A low complexity localization algorithm for mixed far-field and near-field sources," *IEEE Commun. Lett.*, vol. 25, no. 12, pp. 3838–3842, Dec. 2021.
[34] Z. Huang, W. Wang, F. Dong, and D. Wang, "A one-snapshot localization algorithm for mixed far-field and near-field sources," *IEEE Commun. Lett.*, vol. 24, no. 5, pp. 1010–1014, May 2020.
[35] Y. Kuznetsov, A. Baev, M. Konovalyuk, A. Gorbunova, and J. A. Russer, "Autocorrelation analysis and near-field localization of the radiating sources with cyclostationary properties," *IEEE Trans. Electromagn. Compat.*, vol. 62, no. 5, pp. 2186–2195, Oct. 2020.
[36] B. Laufer-Goldshtein, R. Talmon, and S. Gannot, "Semi-supervised source localization on multiple manifolds with distributed microphones," *IEEE Trans. Acoust., Speech, Signal Process.*, vol. 25, no. 7, pp. 1477–1491, Jul. 2017.
[37] B. Laufer-Goldshtein, R. Talmon, and S. Gannot, "Manifold-based Bayesian inference for semi-supervised source localization," in *Proc. IEEE Int. Conf. Acoust., Speech Signal Process. (ICASSP)*, Mar. 2016, pp. 6335–6339.
[38] B. Laufer-Goldshtein, R. Talmon, and S. Gannot, "Semi-supervised sound source localization based on manifold regularization," *IEEE Trans. Acoust., Speech, Signal Process.*, vol. 24, no. 8, pp. 1393–1407, Aug. 2016.
[39] K. Weisberg, S. Gannot, and O. Schwartz, "An online multiple-speaker DOA tracking using the CappÉ-moulines recursive expectation-maximization algorithm," in *Proc. IEEE Int. Conf. Acoust., Speech Signal Process. (ICASSP)*, May 2019, pp. 656–660.
[40] R. Opochinsky, B. Laufer-Goldshtein, S. Gannot, and G. Chechik, "Deep ranking-based sound source localization," in *Proc. IEEE Workshop Appl. Signal Process. Audio Acoust. (WASPAA)*, Oct. 2019, pp. 283–287.
[41] B. Laufer-Goldshtein, R. Talmon, and S. Gannot, "Speaker tracking on multiple-manifolds with distributed microphones," in *Proc. Int. Conf. Latent Variable Anal. Signal Separat.* Berlin, Germany: Springer, 2017, pp. 59–67.
[42] X. Li, Y. Ban, L. Girin, X. Alameda-Pineda, and R. Horaud, "Online localization and tracking of multiple moving speakers in reverberant environments," *IEEE J. Sel. Topics Signal Process.*, vol. 13, no. 1, pp. 88–103, Mar. 2019.
[43] S. Gannot and T. G. Dvorkind, "Microphone array speaker localizers using spatial–temporal information," *EURASIP J. Adv. Signal Process.*, vol. 2006, no. 1, p. 174, Dec. 2006.
[44] B. Laufer, R. Talmon, and S. Gannot, "Relative transfer function modeling for supervised source localization," in *Proc. IEEE Workshop Appl. Signal Process. Audio Acoust.*, Oct. 2013, pp. 1–4.
[45] X. Li, L. Girin, R. Horaud, and S. Gannot, "Multiple-speaker localization based on direct-path features and likelihood maximization with spatial sparsity regularization," *IEEE/ACM Trans. Audio, Speech, Language Process.*, vol. 25, no. 10, pp. 1997–2012, Oct. 2017.

[46] X. Li, L. Girin, R. Horaud, and S. Gannot, "Estimation of the direct-path relative transfer function for supervised sound-source localization," *IEEE/ACM Trans. Audio, Speech, Language Process.*, vol. 24, no. 11, pp. 2171–2186, Nov. 2016.
[47] B. Rafaely, "Analysis and design of spherical microphone arrays," *IEEE Trans. Speech Audio Process.*, vol. 13, no. 1, pp. 135–143, Jan. 2005.
[48] E. G. Williams, *Fourier Acoustics: Sound Radiation and Nearfield Acoustical Holography*. San Francisco, CA, USA: Academic, 1999.
[49] D. B. Ward and T. D. Abhayapala, "Reproduction of a plane-wave sound field using an array of loudspeakers," *IEEE Trans. Speech Audio Process.*, vol. 9, no. 6, pp. 697–707, Sep. 2001.
[50] Y. Hu, P. N. Samarasinghe, G. Dickins, and T. D. Abhayapala, "Modeling the interior response of real loudspeakers with finite measurements," in *Proc. 16th Int. Workshop Acoustic Signal Enhancement (IWAENC)*, Sep. 2018, pp. 16–20.
[51] Y. Hu, P. N. Samarasinghe, T. D. Abhayapala, and G. Dickins, "Modeling characteristics of real loudspeakers using various acoustic models: Modal-domain approaches," in *Proc. IEEE Int. Conf. Acoust., Speech Signal Process. (ICASSP)*, May 2019, pp. 561–565.
[52] Y. Hu, P. N. Samarasinghe, T. D. Abhayapala, and S. Gannot, "Unsupervised multiple source localization using relative harmonic coefficients," in *Proc. IEEE Int. Conf. Acoust., Speech Signal Process. (ICASSP)*, May 2020, pp. 571–575.
[53] D. Khaykin and B. Rafaely, "Coherent signals direction-of-arrival estimation using a spherical microphone array: Frequency smoothing approach," in *Proc. IEEE Workshop Appl. Signal Process. Audio Acoust.*, Oct. 2009, pp. 221–224.
[54] R. O. Schmidt, "Multiple emitter location and signal parameter estimation," *IEEE Trans. Antennas Propag.*, vol. AP-34, no. 3, pp. 276–280, Mar. 1986.
[55] O. J. Famoriji and T. Shongwe, "Electromagnetic machine learning for estimation and mitigation of mutual coupling in strongly coupled arrays," *ICT Exp.*, to be published, doi: 10.1016/j.icte.2021.10.009.
[56] B. Rafaely, *Fundamentals of Spherical Array Processing*, vol. 8. Berlin, Germany: Springer, 2015.

OLUWOLE JOHN FAMORIJI (Member, IEEE) received the B.Tech. degree in electrical and electronic engineering from the Ladoke Akintola University of Technology, Ogbomosho, Nigeria, in 2009, the M.Eng. degree in communications engineering from the Federal University of Technology Akure, Akure, Nigeria, in 2014, and the Ph.D. degree in electronic science and technology from the University of Science and Technology of China (USTC), Hefei, China, in 2019. His research interests include signals and systems, array processing, and antenna and propagation. He was a recipient of one of the Best Papers and Oral Presentation Award of the 2018 IEEE International Conference on Integrated Circuits and Technology Applications (ICTA), Beijing. He also received the 2016 Innovation Spirit Award of the Micro/Nano Electronics System Integration Center and the Institute of Microelectronics Electronics Chinese Academy of Science (MESIC-IMECAS).

THOKOZANI SHONGWE (Senior Member, IEEE) received the B.Eng. degree in electronic engineering from the University of Swaziland, Swaziland, in 2004, the M.Eng. degree in telecommunications engineering from the University of the Witwatersrand, South Africa, in 2006, and the D.Eng. degree from the University of Johannesburg, South Africa, in 2014. He is currently an Associate Professor with the Department of Electrical and Electronic Engineering Technology, University of Johannesburg. His research interests include communications, error correcting coding, power-line communications, cognitive radio, smart grid, visible light communications, machine learning, and artificial intelligence. He was a recipient of the 2014 University of Johannesburg Global Excellence Stature (GES) Award, which was awarded to him to carry out his postdoctoral research at the University of Johannesburg. He was a recipient of the TWAS-DFG Cooperation Visits Program funding to do research in Germany, in 2016. Other awards that he has received in the past are the Post-Graduate Merit Award Scholarship to pursue his master's degree at the University of the Witwatersrand, in 2005, which is awarded on a merit basis. In the year 2012, he (and his coauthors) received an Award of the Best Student Paper at the IEEE ISPLC 2012 (Power Line Communications Conference) in Beijing, China.